Electronic supplementary information

Suppression of polysulfides shuttling with separator modified by spontaneously polarized bismuth ferrite for high performance lithium-sulfur battery

Hao Cheng [a], Huayun Liu [a], Han Jin [a], Ning Cai [a], Cheng Gao [a], Sihan Zhao* [b], Miao Wang * [a]

Zhejiang Province key Laboratory of Quantum Technology and Device, Department of Physics, Zhejiang University, Hangzhou 310027, P. R. China.

Department of Physics, University of California at Berkeley, Berkeley, California 94720, USA.

* Correspondence should be addressed to: sihanzhao88@berkeley.edu and miaowang@zju.edu.cn

Tab. S1 Lattice parameters of $BiFeO_3$ (BFO#2) obtained by Rietveld refinement.

$BiFeO_3$ (BFO#2)	a=5.58243	b=5.58243	c=13.87535	R3c
	α=90.0000	β=90.0000	γ=120.0000	
	X	Y	Z	Occ.
Bi	0.0000	0.0000	0.0000	1.0000
Fe	0.0000	0.0000	0.2215	1.0000
O	0.4392	0.0045	0.9517	1.0000

Tab. S2 The impedance parameters for the cell with PP, GO/AB@PP and BFO/GO/AB@PP separators.

Separators	State	R_0 (Ω)	R_{ct1} (Ω)	R_{ct2} (Ω)
PP	Before 1st	7.53	102.43	35.12
	After 600th	5.82	64.25	36.46
GO/AB@PP	Before 1st	7.31	75.53	13.43
	After 600th	5.69	58.43	12.54
BFO/GO/AB@PP	Before 1st	6.76	62.87	12.85
	After 600th	5.40	45.38	9.67

Tab. S3 Comparison of layer thickness/mass, sulfur content/mass loading and areal capacity between our BFO/GO/AB@PP separator and functional separator designs in recent works.

Layer materials	Layer thickness (μm)	Layer mass (mg cm^{-2})	Sulfur content in cathode (%)	Sulfur loading (mg cm^{-2})	Current density (C)	Areal capacity (mAh cm^{-2})	Ref.
BFO/GO/AB	25	0.48	80%	5.6	0.1	5.1	**This work**
Sb_2Se_{3-x}/rGO	32	0.5	70%	8.1	0.1	7.46	1
Fe_3C/CNF	105	2.25	70%	2.6	0.12	0.65	2
TiO_2/CNF	35	0.55	60%	2.0	0.1	2.40	3
oPANVP/$SnCl_2$	185	0.6	63%	3.0	0.2	3.09	4
$Li_4Ti_5O_{12}$@Graphene	35	0.35	60%	1.1	0.1	1.55	5
MOF@GO	~ 20	~	70%	0.8	0.2	0.86	6
Mesoporous carbon	27	0.5	70%	1.55	0.2	2.14	7
Light-weight Carbon (Super P)	20	0.2	60%	1.3	0.2	1.80	8

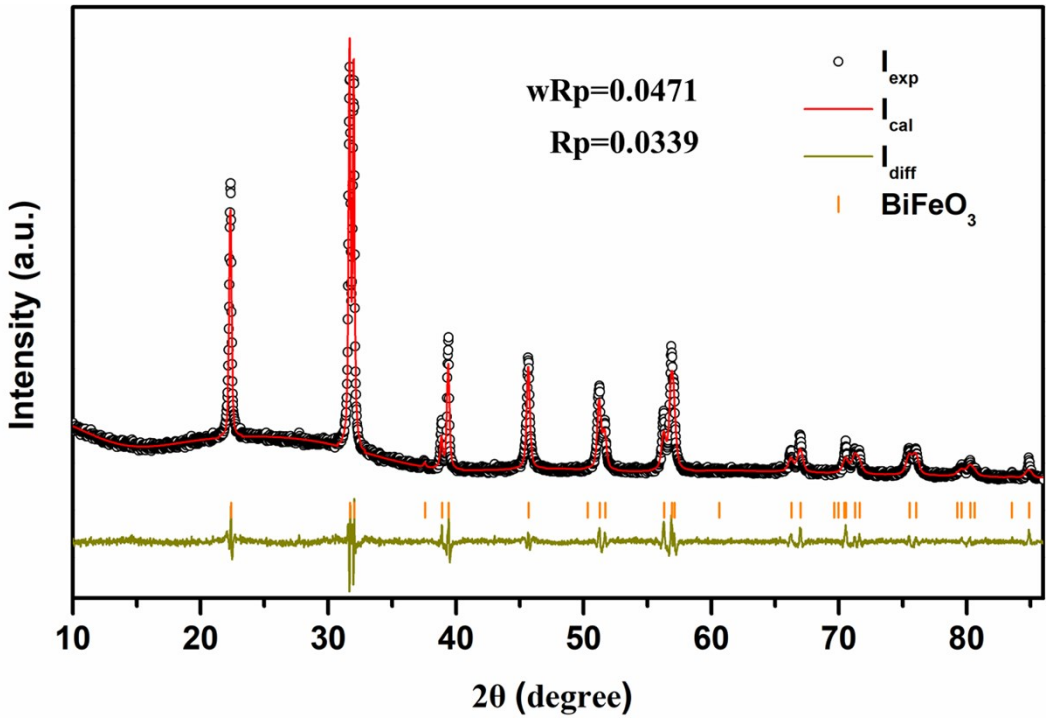

Fig. S1 Experimental, calculated, difference XRD patterns of $BiFeO_3$ (BFO#2) particles.

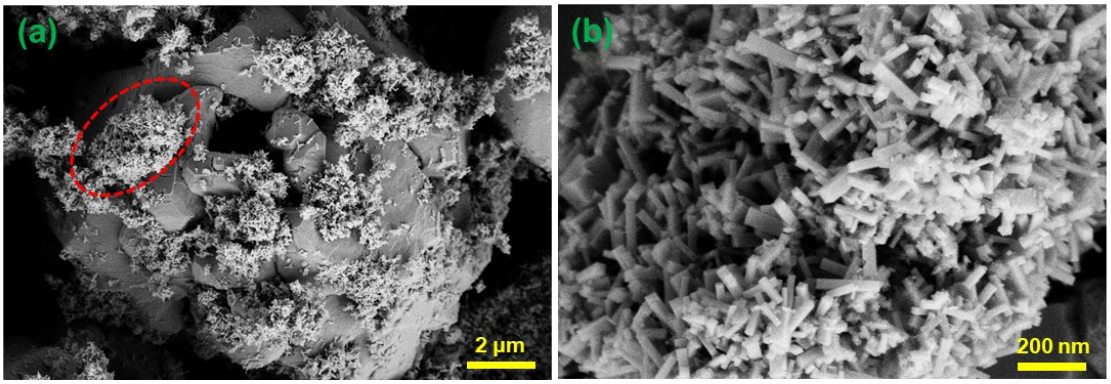

Fig. S2 (a) SEM image of BFO#0, (b) high-resolution SEM image of red circle in (a).

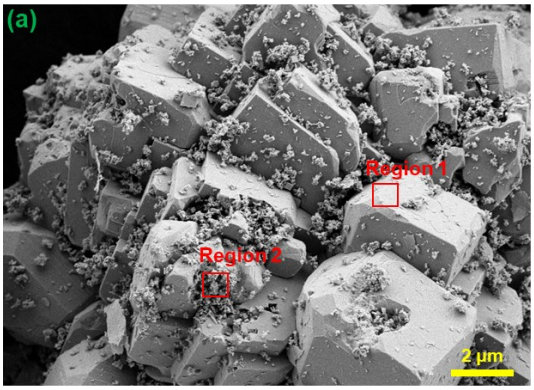

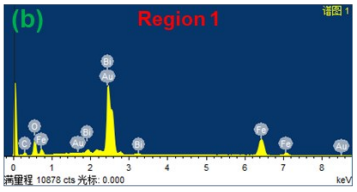

(c) element	Atomic percentage (%)
C K	15.71
O K	55.94
Fe K	13.64
Au M	0.78
Bi M	13.94

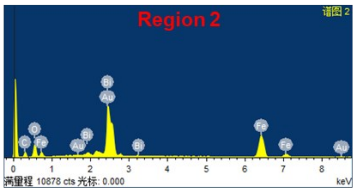

element	Atomic percentage (%)
C K	32.53
O K	41.10
Fe K	16.18
Au M	0.81
Bi M	9.38

Fig. S3 (a) SEM image of BFO#1, (b) EDS spectrum and (c) atomic percentage of region 1 and region 2 in (a), respectively.

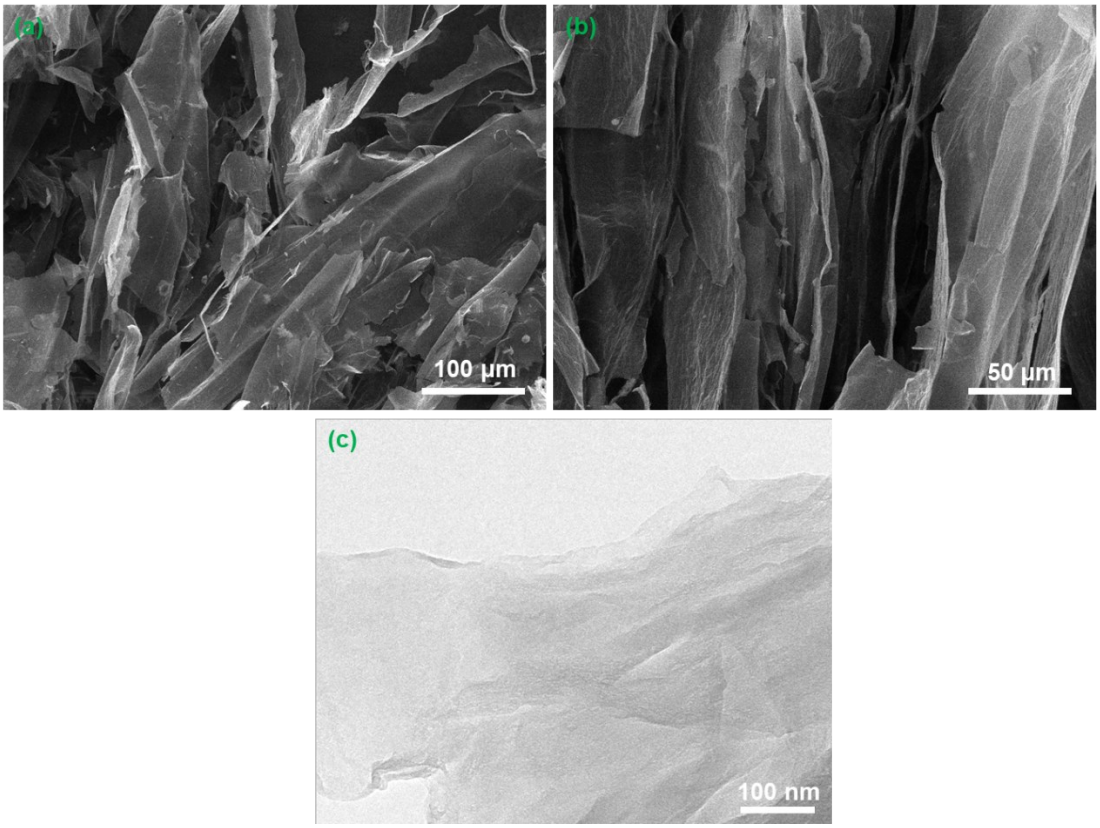

Fig. S4 (a, b) SEM and (c) TEM images of GO.

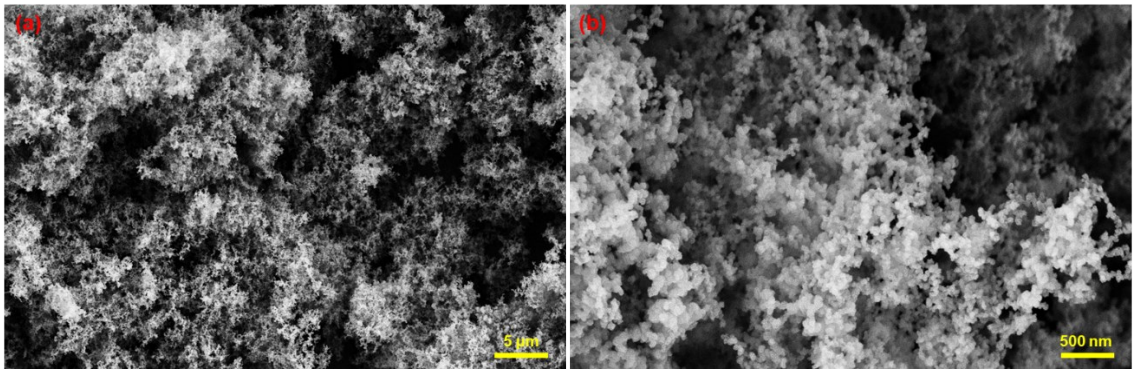

Fig. S5 (a, b) SEM images of AB.

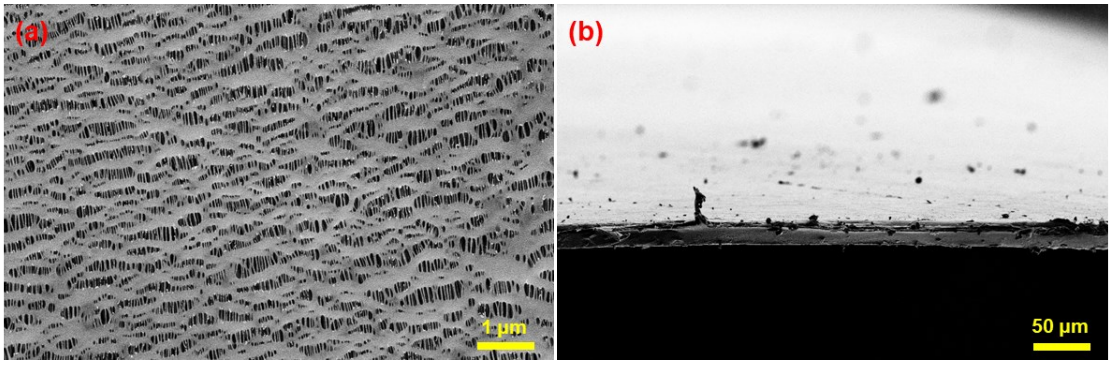

Fig. S6 (a) Top-view and (b) cross-section SEM images of pristine PP separator.

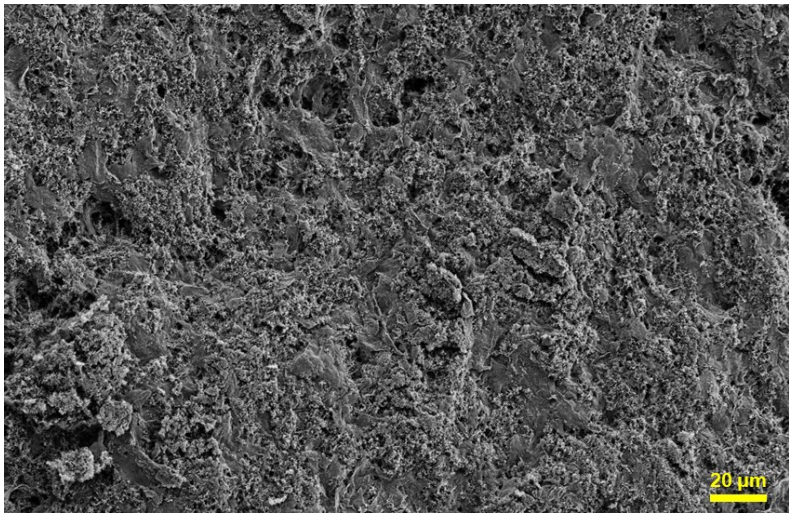

Fig. S7 Top-view SEM image of BFO/GO/AB/PP separator.

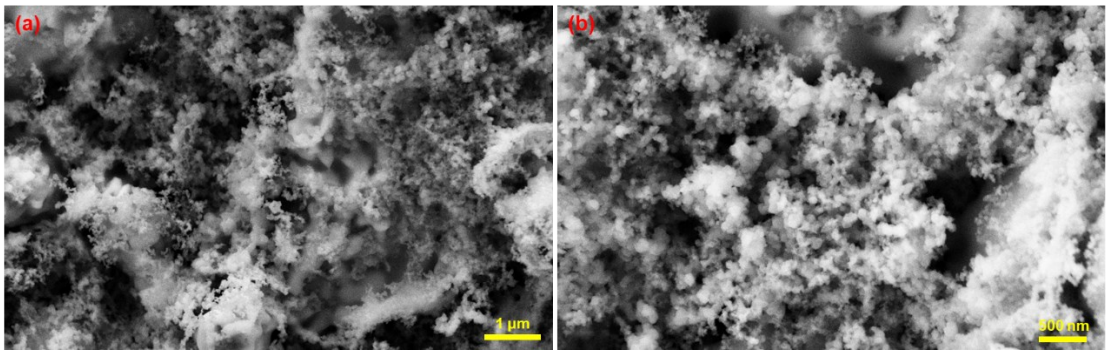

Fig. S8 (a, b) SEM images of C/S composite.

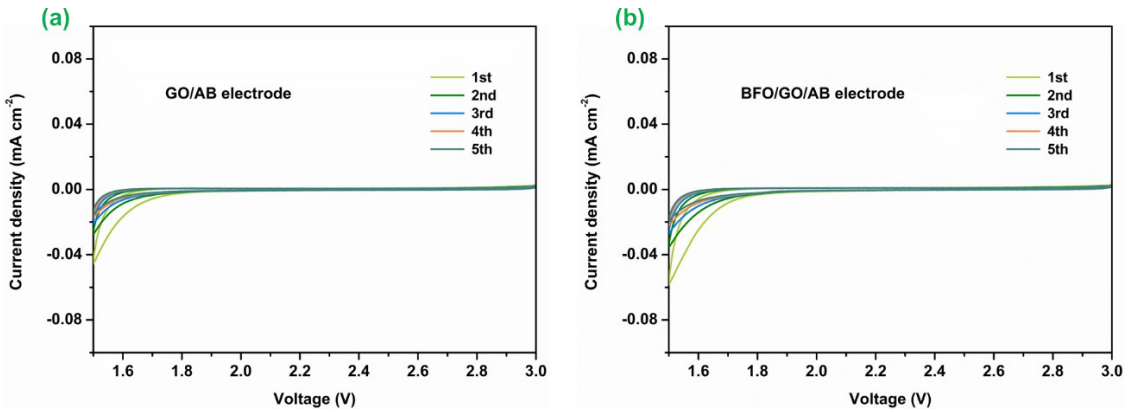

Fig. S9 CV curves of (a) GO/AB electrode and (b) BFO/GO/AB electrode at a scanning rate of 0.1 mV s^{-1}.

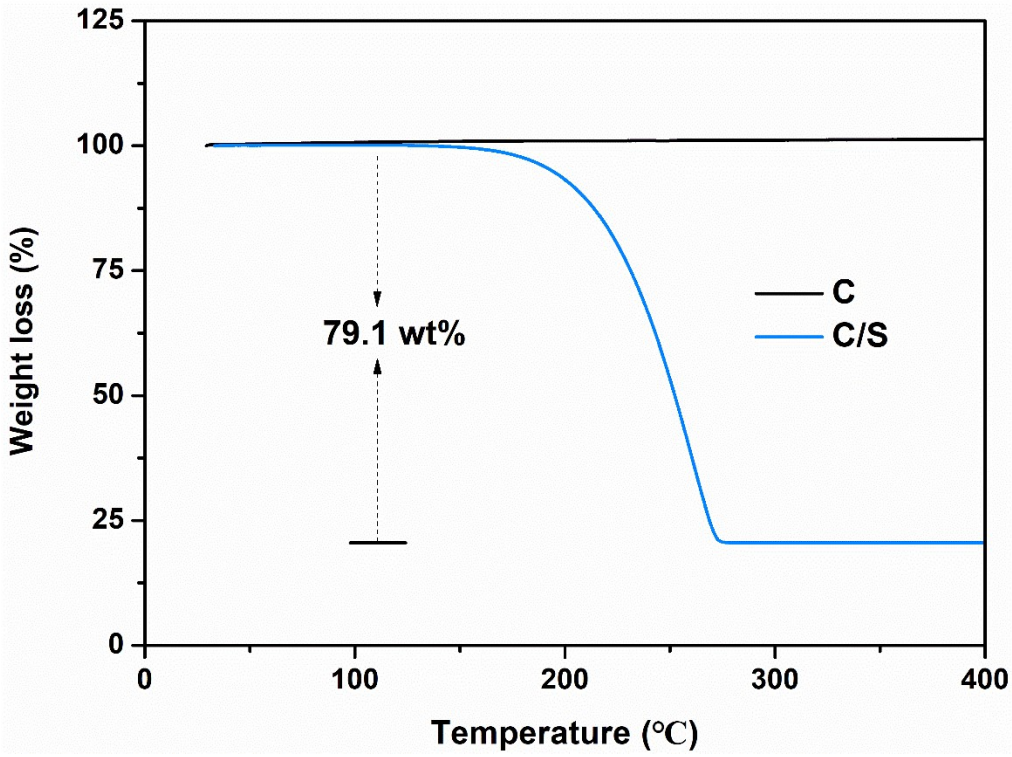

Fig. S10 TGA curves of C and C/S composite.

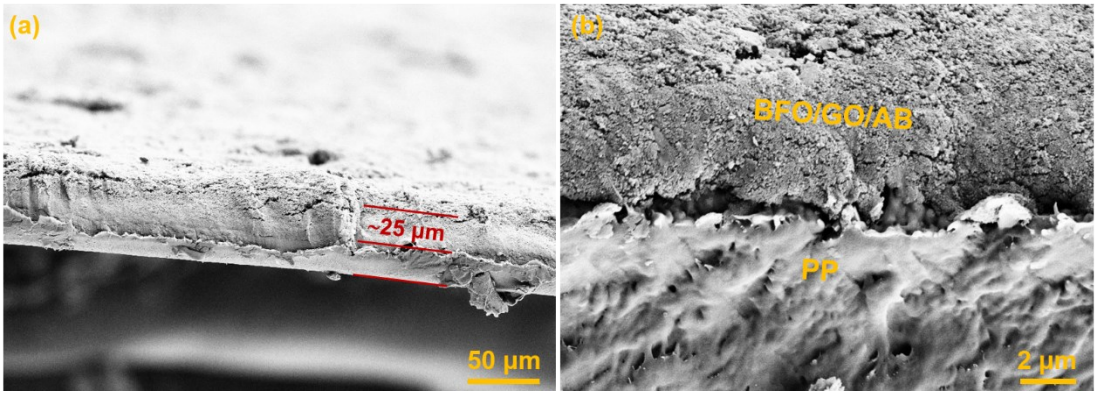

Fig. S11 (a,b) SEM images of BFO/GO/AB@PP separator after 600 cycles at 0.2 C.

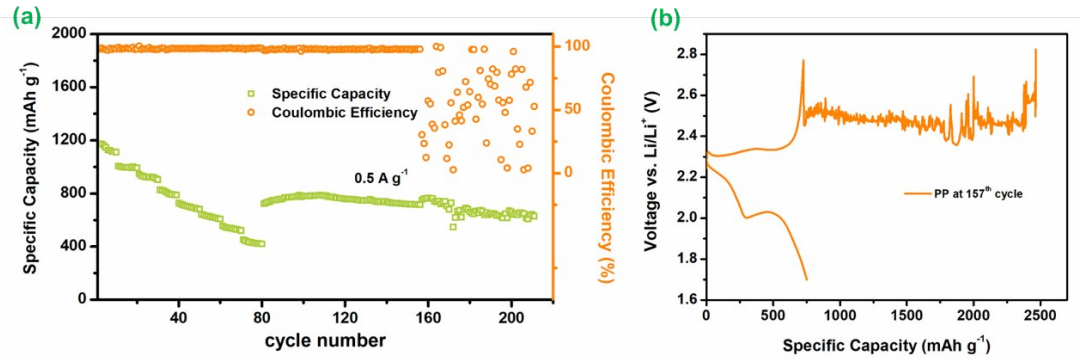

Fig. S12 (a) Rate performance and (b) charge-discharge curves at 157th cycle for the cell with pristine PP separator.

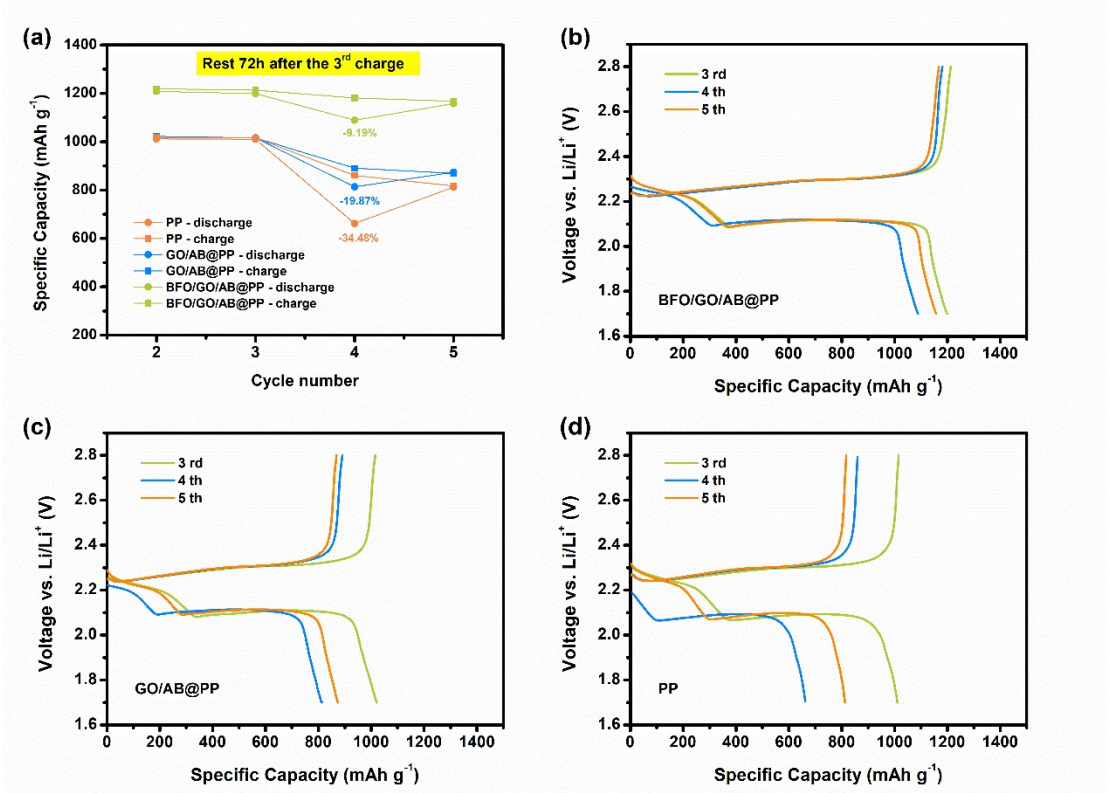

Fig. S13 (a) Cycling performance at 0.2 C with a sulfur loading of 2.0 mg cm^{-2}, the cells were rested for 72 h before the 4^{th} discharge. (b-d) The 3^{rd}, 4^{th} and 5^{th} charge-discharge curves of the cells with BFO/GO/AB@PP, GO/AB@PP and PP separators, respectively.

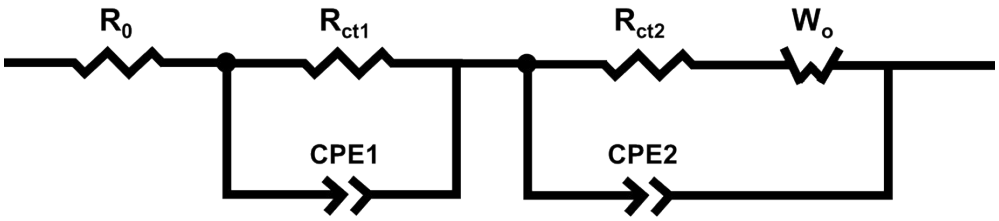

Fig. S14 The fitted equivalent circuit model.

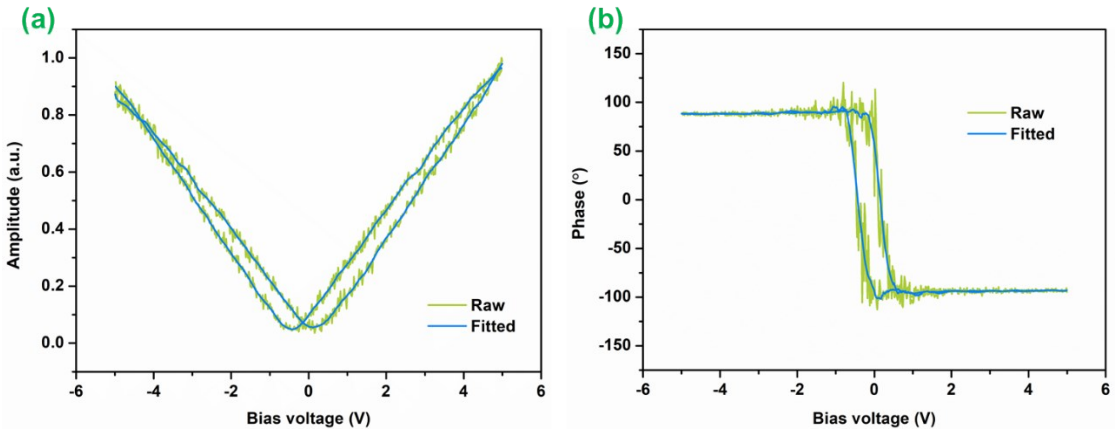

Fig. S15 PFM hysteresis loops of (a) amplitude and (b) phase for BFO/GO/AB@PP separator after cycled.

Reference

1. Y. Tian, G. Li, Y. Zhang, D. Luo, X. Wang, Y. Zhao, H. Liu, P. Ji, X. Du and J. Li, *Adv. Mater.*, 2020, 32, 1904876.
2. J.-Q. Huang, B. Zhang, Z.-L. Xu, S. Abouali, M. A. Garakani, J. Huang and J.-K. Kim, *J. Power Sources*, 2015, 285, 43-50.
3. G. Liang, J. Wu, X. Qin, M. Liu, Q. Li, Y.-B. He, J.-K. Kim, B. Li and F. Kang, *ACS Appl. Mater. Interfaces*, 2016, 8, 23105-23113.
4. E. C. Cengiz, O. Ozturk, S. H. Soytas and R. Demir-Cakan, *J. Power Sources*, 2019, 412, 472-479.
5. Y. Zhao, M. Liu, W. Lv, Y.-B. He, C. Wang, Q. Yun, B. Li, F. Kang and Q.-H. Yang, *Nano Energy*, 2016, 30, 1-8.
6. S. Bai, X. Liu, K. Zhu, S. Wu and H. Zhou, *Nat. Energy*, 2016, 1, 1-6.
7. J. Balach, T. Jaumann, M. Klose, S. Oswald, J. Eckert and L. Giebeler, *Adv. Funct. Mater.*, 2015, 25, 5285-5291.
8. S. H. Chung and A. Manthiram, *Adv. Funct. Mater.*, 2014, 24, 5299-5306.